Few-Body Systems manuscript No.
(will be inserted by the editor)

D. Blume

Efimov physics and the three-body parameter for shallow van der Waals potentials

Received: date / Accepted: date

Abstract Extremely weakly-bound three-boson systems are predicted to exhibit intriguing universal properties such as discrete scale invariance. Motivated by recent experimental studies of the ground and excited helium trimers, this work analyzes the three-body parameter and the structural properties of three helium atoms as the s-wave scattering length is tuned artificially. Connections with theoretical and experimental studies of the Efimov scenario as it pertains to cold atom systems are made.

1 Introduction

In 1970, Vitaly Efimov considered three identical bosons with short-range two-body interactions [1]. In the limit that each of the three pairs is just short of supporting a two-body bound state, Efimov predicted that the three-body system would support infinitely many three-body states with geometrically spaced binding energies. Moreover, as the two-body attraction is increased, the most weakly-bound three-body states become unbound. Efimov's counterintuitive predictions are based on ordinary non-relativistic quantum mechanics and have stimulated concerted theoretical and experimental efforts [2; 3; 4; 5; 6; 7; 8; 9; 10; 11; 12; 13; 14; 15; 16; 17; 18; 19; 20]. The geometric spacing of the three-body bound states in the regime where the two-body system is just short of supporting a shallow two-body bound state (i.e., when the absolute value of the two-body s-wave scattering length a is infinitely large) can be understood as a consequence of a discrete scale invariance or an infrared limit cycle [8]. Importantly, the changes of the three-body energies with increasing and decreasing two-body attraction (i.e., for finite positive and finite negative s-wave scattering lengths) are also captured by the universal theory.

Intriguingly, Efimov's scenario is independent of the details of the underlying two-body interactions. It should apply if the s-wave scattering length is much larger than the other two-body length scales such as the effective range. Provided this is the case, the three-body system is, to a good approximation, governed by just two parameters, the s-wave scattering length and a three-body parameter. Over the past few years, much effort has been devoted to understanding what determines the value of the three-body parameter for three-body systems that interact through pairwise two-body van der Waals potentials with long-range $-C_6 r^{-6}$ tail [21]. While it was long thought that the three-body parameter could take any value, it is now believed that two-body van der Waals universality plays a crucial role in understanding the three-body parameter for atomic three-body systems [22; 23; 24; 25; 26; 27].

The universal zero-range theory does not make predictions about the value of the three-body parameter. Using $\bar{\kappa}^{(n^*)}$, where $\bar{\kappa}^{(n^*)}$ denotes the binding momentum of the n^*th Efimov trimer with infinitely large s-wave scattering length (there exists an infinity of Efimov states and n increases with decreasing binding), to "anchor" the three-body spectrum, the three-body energy $E_t^{(n)}$ ($E_t^{(n)} \leq 0$) of

Department of Physics and Astronomy, Washington State University, Pullman, Washington 99164-2814, USA

Table 1 Summary of theoretical literature results for single channel two-body potentials. The values reported by Wang *et al.* [24] are obtained for a two-body hardcore potential with $-C_6 r^{-6}$ tail that supports a single two-body zero-energy s-wave bound state at unitarity; these values are found to agree quite well with those obtained for Lenard-Jones potentials that support many two-body s-wave bound states [24]. The values reported by Naidon *et al.* [26] are obtained for separable two-body potential models that are designed to mimick the behavior of two-body Lenard-Jones potentials with varying number of two-body s-wave bound states; the separable model is reported to reproduce the binding wave number of the full model potentials with less than about 10 % error [26]. The zero-range (ZR) theory provides information about the product $\bar{\kappa}^{(n)}\bar{a}^{(n)}$ but not about the values of $\bar{\kappa}^{(n)}$ or $\bar{a}^{(n)}$; the zero-range theory results are independent of n.

	$\bar{\kappa}^{(1)} r_6$	$\bar{a}^{(1)}/r_6$	$\bar{\kappa}^{(1)}\bar{a}^{(1)}$
Wang *et al.* [24]	0.226(2)	−9.73(3)	−2.20(2)
Naidon *et al.* [26]	0.187(1)	−10.85(1)	−2.03(1)
ZR theory [28]			−1.50763

the nth Efimov trimer is determined by the radial law [8]

$$|E_t^{(n)}| + \frac{\hbar^2}{ma^2} = [\exp(-2\pi/s_0)]^{n-n^*} \exp(\Delta(\xi)/s_0) \frac{\hbar^2(\bar{\kappa}^{(n^*)})^2}{m}, \tag{1}$$

where s_0 is equal to 1.00624, $\Delta(\xi)$ is a universal function whose parameterization is given in Ref. [8], and $\tan\xi = -\kappa^{(n)}a$ with $\kappa^{(n)} = (m|E_t^{(n)}|)^{1/2}/\hbar$. The angle ξ goes from $-\pi/4$ to $-\pi$: $-\pi/4$ corresponds to the points where the energy of the trimer is equal to that of the dimer, $-\pi/2$ corresponds to infinitely large s-wave scattering lengths, and $-\pi$ corresponds to the points where the trimer energy is equal to zero. Equation (1) implies the following relations [8]:

$$\bar{\kappa}^{(n)}/\bar{\kappa}^{(n+1)} = 22.6944, \tag{2}$$

$$\bar{a}^{(n)}/\bar{a}^{(n+1)} = (22.6944)^{-1}, \tag{3}$$

and [8; 28]

$$\bar{\kappa}^{(n)}\bar{a}^{(n)} = -1.50763. \tag{4}$$

Here, $\bar{a}^{(n)}$ denotes the s-wave scattering length at which the nth Efimov trimer becomes unbound, i.e., the scattering length corresponding to $\xi = -\pi$. Since $\bar{a}^{(n)}$ and $\bar{\kappa}^{(n)}$ are related through Eq. (4), the radial law can be rewritten in terms of $\bar{a}^{(n^*)}$ instead of $\bar{\kappa}^{(n^*)}$; in fact, the radial universal zero-range theory law can be rewritten in infinitely many ways since all three-body energies are related to each other.

The Efimov spectrum of three-body systems interacting through two-body van der Waals potentials starts at a finite negative energy since the short-range two-body repulsion, which is a consequence of the Pauli exclusion principle, provides a "natural regularization" or energy cutoff. Labeling the most strongly-bound Efimov trimer by $n = 1$ [29] (note that there is a certain ambiguity in deciding where the ladder of Efimov states starts for systems with finite-range interactions; see also below), Table 1 summarizes the results of two different theoretical studies for $\bar{\kappa}^{(1)}$, $\bar{a}^{(1)}$ and $\bar{\kappa}^{(1)}\bar{a}^{(1)}$ [24; 26]. It can be seen that $\bar{\kappa}^{(1)}\bar{a}^{(1)}$ for the van der Waals trimer is by 46% [24] and 35% [26] larger than the universal zero-range value, suggesting that finite-range corrections are non-negligible (see also Refs. [30; 31; 32; 33; 34]). This suggests that $\bar{\kappa}^{(1)}$ and $\bar{a}^{(1)}$ should not be considered equally good three-body parameters (see also Ref. [36]). We argue below that $\bar{\kappa}^{(1)}$ provides the better choice, i.e., it provides a more reliable anchor for the three-body spectrum. The three-body parameter for finite-range two-body potentials has recently been linked to the onset of a renormalization group limit cycle [35].

We present calculations for three-body systems interacting through shallow two-body van der Waals potentials and analyze the energy spectrum and structural properties. Our study is motivated by a large body of cold atom related work [4; 5; 6; 7; 8; 9; 10; 11; 12; 13; 14; 15; 16; 17; 18; 19; 20] and recent experimental measurements of the structural properties of the helium trimer ground and excited states [37; 38]. The ground state of the helium trimer is, generally, considered not to be an Efimov state while the helium trimer excited state is considered to be an Efimov state [39; 40; 41; 42]. Our calculations are related to literature results, some of which are summarized in Table 1. A simple—perhaps not unexpected—take-home message of our work is that the size of the trimer plays an important role in determining how universal its properties are.

Table 2 Numerical results (this work) for three-body systems interacting through shallow single-channel two-body potentials, which support one zero-energy s-wave bound state at unitarity. The van der Waals length r_6 for the two-body potential He-He(scale) changes as the scale factor λ is changed while the van der Waals length for the two-body potentials He-He(SR) and Lenard-Jones (LJ) remains unchanged as the short-range behavior of the two-body potentials is changed.

	$\bar{\kappa}^{(1)}r_6$	$\bar{a}^{(1)}/r_6$	$\bar{\kappa}^{(1)}\bar{a}^{(1)}$	$\bar{\kappa}^{(2)}r_6$	$\bar{a}^{(2)}/r_6$	$\bar{\kappa}^{(2)}\bar{a}^{(2)}$	$\bar{\kappa}^{(1)}/\bar{\kappa}^{(2)}$	$\bar{a}^{(1)}/\bar{a}^{(2)}$
He-He(scale)	0.222	−9.80	−2.12	0.00947	−166.	−1.57	23.4	$(17.3)^{-1}$
He-He(SR)	0.218	−9.88	−2.15	0.00928	−169.	−1.57	23.5	$(17.1)^{-1}$
LJ	0.230	−9.49	−2.18	0.00981	−160.	−1.57	23.4	$(16.8)^{-1}$

2 Results

This section considers trimers interacting through a sum of two-body potentials λV_{He-He}; we refer to this interaction model as He-He(scale). For V_{He-He}, we use the most recent helium-helium potential with retardation by Cencek *et al.* [46]. The multiplication factor λ is a scaling parameter that allows for the tuning of the s-wave scattering length. A value of $\lambda = 1$ corresponds to the true helium-helium system with two-body s-wave scattering length $a = 170.9(1.7)a_0$ [47], while a value greater (smaller) than one corresponds to $a > 170.9a_0$ ($a < 170.9a_0$), where a_0 denotes the Bohr radius. The scaling of the helium-helium potential has been used extensively in the literature [39; 41; 48; 49; 50]. It is important to note that the overall scaling factor does not only change the s-wave scattering length but also the van der Waals length r_6 [21],

$$r_6 = \frac{1}{2}\left(\frac{m\lambda C_6}{\hbar^2}\right)^{1/4}, \tag{5}$$

and the effective range r_e. Here, m denotes the atomic mass, $m = 7296.2996m_e$ (m_e is the electron mass), and C_6 the van der Waals coefficient of the helium-helium potential. For $\lambda = 1$, we have $r_6 = 5.08050a_0$.

The relative three-body Schrödinger equation is solved using the hyperspherical coordinate approach [39; 51]. Our calculations employ 12 adiabatic channels and yield energies that should be converged to about 1%. Figure 1 shows the energy (more precisely, it shows the quantity $-|E_t^{(n)}|^{1/4}$) for the ground (circles) and excited (squares) states as a function of $sign(a)|a|^{-1/2}$. As already mentioned, the helium trimer ground state is, generally, not considered to be an Efimov state, suggesting that it would be appropriate to label the first excited state by $n = 1$. However, in what follows we analyze the ground and excited states, using the labeling $n = 1$ for the ground state and $n = 2$ for the excited state. We find for the ground and first excited states $\bar{\kappa}^{(1)} \approx 0.0439a_0^{-1}$, $\bar{a}^{(1)} \approx -48.31a_0$, $\bar{\kappa}^{(2)} \approx 0.00188a_0^{-1}$, and $\bar{a}^{(2)} \approx -834a_0$. Our values for $\bar{\kappa}^{(n)}$ and $\bar{a}^{(n)}$ agree at the few percent level with those reported in the literature for other scaled helium-helium interaction models [49].

The row labeled He-He(scale) in Table 2 reexpresses $\bar{a}^{(n)}$ and $\bar{\kappa}^{(n)}$ in terms of the van der Waals length r_6 and its inverse. Using this scale, $\bar{\kappa}^{(1)}$ and $\bar{a}^{(1)}$ for the He-He(scale) interaction model take on values similar to those reported in Table 1, suggesting that the C_7 and higher-order van der Waals coefficients play a negligible role. Importantly, the values of the ratio $\bar{\kappa}^{(1)}/\bar{\kappa}^{(2)}$ and the product $\bar{\kappa}^{(2)}\bar{a}^{(2)}$ are close to those of the universal zero-range theory, suggesting that $\bar{\kappa}^{(1)}$, $\bar{\kappa}^{(2)}$ or $\bar{a}^{(2)}$ can be used to anchor the three-body spectrum but not $\bar{a}^{(1)}$. For example, using $n^* = 1$ or 2 in Eq. (1), the energy of the $n = 2$ trimer interacting through He-He(scale) can be reproduced quite accurately by the radial universal zero-range theory law. The energy of the $n = 1$ level, in contrast, is described comparatively poorly by the radial universal zero-range theory law (see, e.g., Ref. [41]). This is illustrated by the solid lines in Fig. 1, which show the universal zero-range energies obtained from the radial law, Eq. (1), using $n^* = 2$. The deviations between the solid line and the circles are one of the reasons why the $n = 1$ state is, generally, not considered to be an Efimov state.

To gain more insight into the universality of weakly-bound trimers interacting through shallow two-body potentials, we consider two other potential models, He-He(SR) and LJ. The model He-He(SR) is based on the potential V_{He-He}. However, as opposed to multiplying by the overall scaling factor λ, we multiply V_{He-He} by a short-range function $f(r)$, which goes to one for large interparticle distances r and thus leaves the van der Waals tail of V_{He-He} unchanged. The function $f(r)$ reads $3 - 4\arctan[(r - 4.75a_0)/l]/\pi$, where l ranges from about $10^{-2}a_0$ to $0.16a_0$ [$f(r)$ changes at $r \approx 4.75a_0$

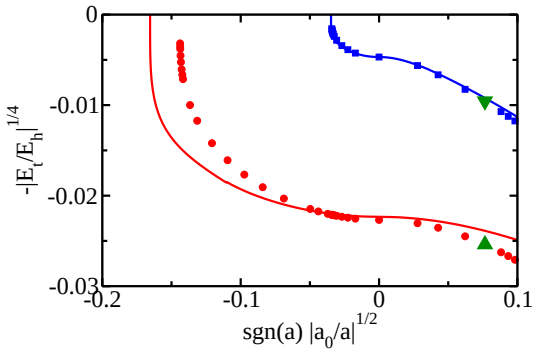

Fig. 1 (Color online) The circles and squares show the energy of the $n = 1$ and 2 trimer states for the He-He(scale) model. The energy of the true helium trimers ($\lambda = 1$) is shown by up and down triangles. For comparison, the solid lines show the $n = 1$ and 2 energies obtained from Eq. (1) using $n^* = 2$. The scattering length a and energy $E_t^{(n)}$ are scaled by the Bohr radius a_0 and the Hartree energy E_h, respectively.

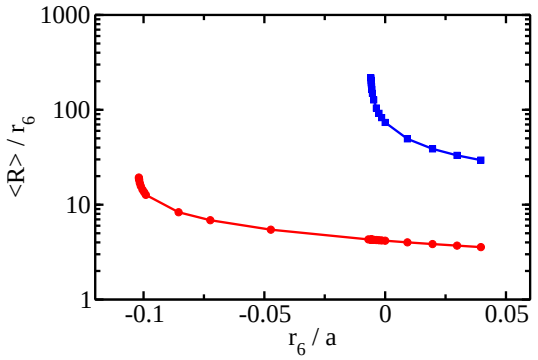

Fig. 2 (Color online) Expectation value $\langle R\rangle$ for the $n = 1$ (circles) and $n = 2$ (squares) trimers interacting through He-He(scale) as a function of $1/a$. The solid lines connect neighboring data points and serve as a guide to the eye.

over the distance l from 5 to 1]. The two-parameter Lenard-Jones (LJ) potential has a fixed $-C_6 r^{-6}$ tail, with the short-range parameters adjusted such that the potential supports one two-body zero-energy s-wave bound state at unitarity. Table 2 summarizes our results for $\bar{\kappa}^{(n)}$ and $\bar{a}^{(n)}$ for these two potential models. Our $n = 1$ results for the LJ model agree with the values read off Fig. 4 of Ref. [24]. It can be seen that $\bar{\kappa}^{(n)}$ and $\bar{a}^{(n)}$ (expressed in terms of r_6), as well as the combinations of $\bar{\kappa}^{(n)}$ and $\bar{a}^{(n)}$, take on similar values for the potential models He-He(SR) and LJ as for the potential model He-He(scale). This is expected in view of the existing literature on three-body van der Waals universality [22; 23; 24; 25; 26; 27]. We return to the results presented in Table 2 for the different interaction models in Sec. 3.

We now discuss selected structural properties, focussing on trimers interacting through He-He(scale). Figure 2 shows the expectation value $\langle R\rangle$ of the hyperradius R as a function of r_6/a for the $n = 1$ (circles) and $n = 2$ (squares) trimers. The hyperradius R, which is defined through $R^2 = (r_{12}^2 + r_{23}^2 + r_{31}^2)/3$ (r_{jk} denotes the interparticle distance between atoms j and k), can be thought of as the average size of the system [52]. For $\lambda = 1$ ($r_6/a = 0.0297$), we find $\langle R\rangle \approx 3.70 r_6$ and $\langle R\rangle \approx 33.1 r_6$ for $n = 1$ and 2, respectively. The value of $\langle R\rangle$ increases for both states with decreasing λ, i.e., decreasing r_6/a. For

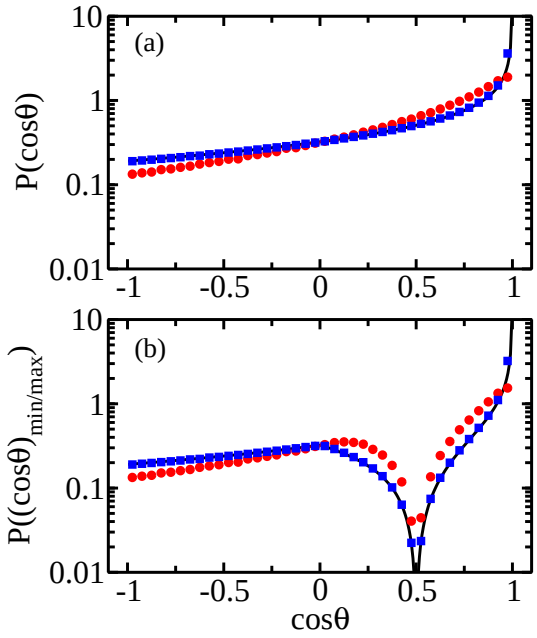

Fig. 3 (Color online) Cos-distributions for $1/a = 0$. Circles and squares show the distributions of the $n = 1$ and 2 states for the He-He(scale) model. For comparison, the solid lines show the distributions obtained using the zero-range theory (note, the solid line is hardly visible for negative $\cos\theta$ values, where it is "covered up" by the squares). Panel (a) shows the cos-distribution obtained by binning the quantity $\cos\theta$ for all three angles, while panel (b) shows the distributions obtained by binning only the smallest $\cos\theta$ ($\cos\theta < 1/2$, corresponding to $\theta > 60$ degrees) or the largest $\cos\theta$ ($\cos\theta > 1/2$, corresponding to $\theta < 60$ degrees) values.

$1/a = 0$, we find $\langle R\rangle \approx 4.17 r_6$ and $\langle R\rangle \approx 73.5 r_6$. Near the three-atom thresholds, i.e., for a slightly larger than $\bar{a}^{(1)}$ and $\bar{a}^{(2)}$, the trimers are quite large. The most weakly-bound $n = 1$ trimer considered ($a \approx -48.37 a_0$, $r_6/a \approx -0.1020$, and $\langle R\rangle \approx 19.3 r_6$) is about 3 orders of magnitude less strongly bound than the corresponding trimer at unitarity while the most weakly-bound $n = 2$ trimer considered ($a \approx -856 a_0$, $r_6/a \approx -0.00589$, and $\langle R\rangle \approx 216 r_6$) is about 2 orders of magnitude less strongly bound than the corresponding trimer at unitarity.

To gain more insight into the structural properties, we calculate the distribution of the cosine of the angle θ, where θ denotes the angle between any two of the three interparticle distance vectors. The results for the He-He(scale) interaction model at unitarity are compared to the universal zero-range theory. Since the universal zero-range theory wave function for infinitely large a is known in analytical form [53; 54], structural properties can be determined by sampling the analytically known density using the Metropolis algorithm. Figure 3(a) shows the distribution $P(\cos\theta)$ for the $n = 1$ and 2 trimers interacting through He-He(scale) (circles and squares) as well as for the trimer described by the universal zero-range theory (solid line). The normalization is chosen such that $\int_{-1}^{1} P(x)dx$ with $x = \cos\theta$ is equal to 1. It can be seen that the $n = 2$ distribution for the finite-range potential is described very well by the zero-range theory. Significant deviations are, however, visible for the $n = 1$ state, which has a notably lower probability for $\cos\theta = \pm 1$, corresponding to angles around 0 and 180 degrees. The deviations are more pronounced in Fig. 3(b), which shows the distributions for the maximum (minimum) value of $\cos\theta$ using the same symbols and line style as in Fig. 3(a). The difference between the $n = 1$ and 2 states reflects the fact that the $n = 1$ state is quite well described by a random cloud model [37] while the $n = 2$ state is best thought of as corresponding, roughly, to a dimer plus atom geometry [55]. Figure 3 indicates that—to be in the universal regime—it is not sufficient to satisfy the inequality $|r_6/a| \ll 1$; in addition, the size of the trimer needs to be much larger than the van der

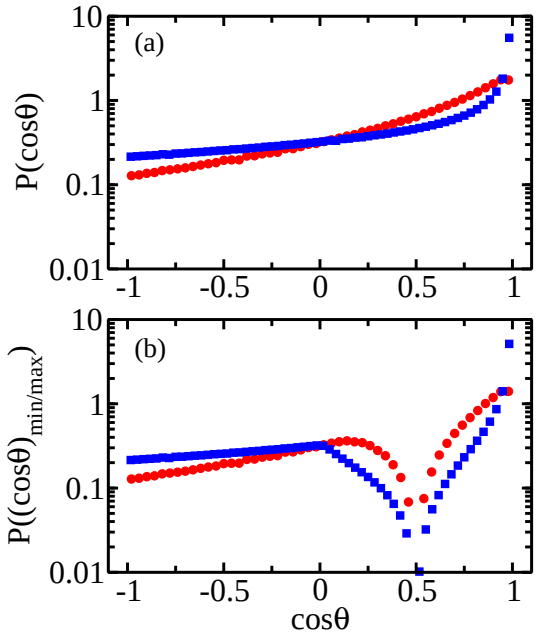

Fig. 4 (Color online) Circles and squares show the cos-distributions of the $n = 1$ and 2 states for the true helium trimer system, i.e., for the He-He(scale) model with $\lambda = 1$. Panel (a) shows the cos-distribution obtained by binning the quantity $\cos\theta$ for all three angles (these distributions are shown, using a different y-axis, for the LM2M2 potential model in Ref. [51]), while panel (b) shows the distributions obtained by binning only the smallest $\cos\theta$ ($\cos\theta < 1/2$) or the largest $\cos\theta$ ($\cos\theta > 1/2$) values.

Waals length scale. For the $n = 1$ state, we have $\langle R\rangle/r_6 \approx 4.17$ [56] (see our earlier discussion); this value is too small for the $n = 1$ state of the He-He(scale) model with infinitely large a to be accurately described by the universal zero-range theory.

Figure 4 shows the cos-distributions for the $n = 1$ (circles) and $n = 2$ (squares) states of the true helium trimer, i.e., for the He-He(scale) model with $\lambda = 1$ [57]. Our result for the $n = 1$ state shown in Fig. 4(a), plotted as a function of θ as opposed to $\cos\theta$, agree with the distribution determined experimentally [37]. Comparison with Fig. 3 shows that the overall behavior of the cos-distributions is unchanged as the s-wave scattering length changes from an infinitely large value to a large positive value of $170.9a_0$. Thus, Fig. 4 supports the notion that the helium trimer ground state does not behave like an Efimov state while the helium trimer excited state does.

Lastly, we consider the negative scattering length side. To meaningfully compare the characteristics of the $n = 1$ and 2 states, Fig. 5 shows the cos-distributions for scattering lengths that are about 2.5 % more negative than the scattering lengths $\bar{a}^{(n)}$ at which the respective trimers become unbound. Figures 5(a) and 5(b) show quite good agreement between the distributions for the $n = 1$ and 2 states near the three-atom threshold, indicating that the $n = 1$ trimer exhibits close to universal structural characteristics in this regime. We interpret this as follows. The finite a/r_6 value (recall, $\bar{a}^{(1)}/r_6 \approx -9.80$) leads to non-universal corrections of $\bar{a}^{(1)}$, as evidenced by the fact that the ratio $\bar{a}^{(2)}/\bar{a}^{(1)}$ deviates by 24% from the universal value. However, since the size of the ground state trimer is large (for the scattering length considered in Fig. 5, we find $\langle R\rangle/r_6 \approx 13.5$), the majority of the trimer density is found in the classically forbidden region and the structural properties resemble those expected for the universal zero-range theory relatively closely.

The above discussion can be summarized as follows. The value of the ratio $\bar{\kappa}^{(1)}/\bar{\kappa}^{(2)}$ is close to the universal zero-range theory prediction. The structural properties of the $n = 1$ state at unitarity, however, are not well described by the universal zero-range theory. Non-universal corrections exist

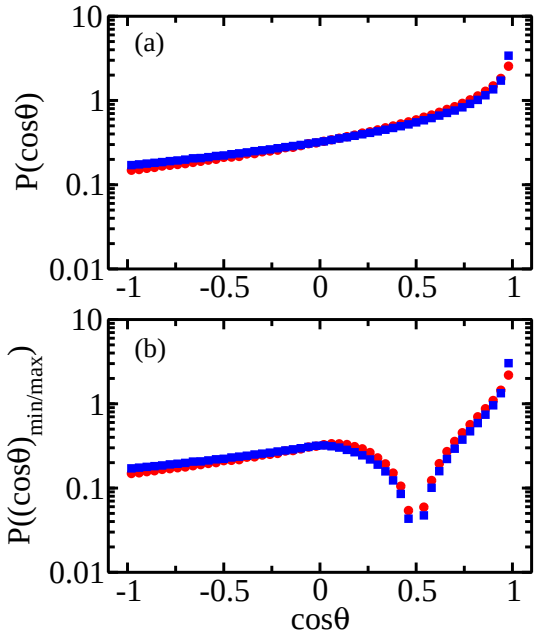

Fig. 5 (Color online) Circles and squares show the cos-distributions of the $n = 1$ and 2 states for He-He(scale) near the three-atom threshold (see text for details). Panel (a) shows the cos-distribution obtained by binning the quantity $\cos\theta$ for all three angles while panel (b) shows the distributions obtained by binning only the smallest $\cos\theta$ ($\cos\theta < 1/2$) or the largest $\cos\theta$ ($\cos\theta > 1/2$) values.

since $\langle R\rangle/r_6$ is, for the $n = 1$ state, only a few times larger than 1. The value of the product $\bar{\kappa}^{(1)}\bar{a}^{(1)}$, in contrast, is not close to the universal zero-range theory prediction. Non-universal corrections exist since $|\bar{a}^{(1)}|/r_e$ is only a few times larger than 1. Yet, the structural properties of the $n = 1$ state in the vicinity of the three-atom threshold follow the expected universal behavior relatively closely. Thus, to estimate the magnitude of the finite-range corrections both $|a|/r_6$ and $\langle R\rangle/r_6$ have to be considered.

3 Summary and Outlook

The study of weakly-bound three-body states remains an active area of research, with implications for a wide range of research thrusts including atomic, nuclear, particle and condensed matter physics. This paper considered atomic three-body systems with shallow two-body van der Waals interactions in the regime where the absolute value of the two-body s-wave scattering length is large compared to the van der Waals length or effective range; note, r_6 and r_e are, for two-body potentials with pure $-C_6 r^{-6}$ tail, related through $r_e = 2.78947 r_6$.

The ground and excited states of the helium trimer interacting through the most accurate realistic helium-helium potential [46; 47] were investigated. The universality of the helium trimer states, or lack thereof, was analyzed by two different means. First, the relationship between $\bar{a}^{(n)}$ and $\bar{\kappa}^{(n)}$, obtained by scaling the true helium-helium potential, was compared to the universal zero-range theory prediction. In agreement with earlier studies [39; 40; 41], these results let one conclude that the helium trimer ground state should not be considered an Efimov state while the helium trimer excited state should be. Second, selected structural properties were analyzed. Again, the results let one conclude that the helium trimer ground state should not be considered an Efimov state while the helium trimer excited state should be. The analysis of the structural properties was motivated by experimental advancements that allow for the imaging of the quantum mechanical helium trimer densities via the Coulomb explosion imaging technique [37; 38]. Importantly, the structural properties in the vicinity of $\bar{a}^{(1)}$ (realized by

Table 3 Summary of experimental cold atom results. The results are obtained by analyzing three-body recombination data. The lithium experiments work with a three-component mixture. Reference [36] presents, in our notation, results for $\bar{\kappa}^{(1)}$ and $\bar{\kappa}^{(2)}$. Converting to $\bar{a}^{(n)}$ using Eq. (4), yields the $\bar{a}^{(n)}$ values reported in the Table.

	$\bar{a}^{(1)}/r_6$	$\bar{a}^{(2)}/r_6$	$\bar{a}^{(1)}/\bar{a}^{(2)}$
cesium [58]	$-9.53(11)$	$-200(12)$	$[21.0(1.3)]^{-1}$
lithium [36]	$-7.50(5)$	$-161(1)$	$[21.5(2)]^{-1}$

artificially scaling the two-body He-He potential), where the trimer size $\langle R \rangle$ is much larger than the absolute value of the s-wave scattering length, are described reasonably well by the universal zero-range theory.

It has been suggested that the applicability of the universal scaling law, Eq. (1), can be extended through the introduction of a shift parameter, which accounts for finite-range effects [50]. The resulting modified scaling law has been shown to describe the helium trimer ground state quite accurately. It is an interesting question whether this extension can be generalized to distribution functions, which probe local as opposed to global (averaged) properties of the quantum mechanical probability density.

It is also interesting to attempt to connect our results for trimers interacting through shallow two-body van der Waals potentials with recent ultracold atom studies. While alkali-alkali interactions are multi-channel in nature, ultracold trimers in the vicinity of broad two-body s-wave Feshbach resonances may share similarities with the results obtained for the single-channel models considered in this paper. Table 3 summarizes the results for equal-mass alkali trimers for which two consecutive Efimov features have been observed experimentally. For Cs [58], the value of $\bar{a}^{(1)}/r_6$ agrees well with what has been found theoretically for shallow (Table 2) and deep (Ref. [24]) single-channel van der Waals models. The value of $\bar{a}^{(2)}/r_6$, however, is more negative than what has been found theoretically for the shallow single-channel models (see Table 2), yielding a value of $[\bar{a}^{(1)}/\bar{a}^{(2)}]^{-1}$ that is smaller than the universal zero-range value but larger than the value found in this work. We believe that two-body single-channel van der Waals potentials that support many two-body s-wave bound states would yield a value for $\bar{a}^{(2)}/r_6$ that is close to the $\bar{a}^{(2)}/r_6$ value reported in Table 2 for shallow two-body van der Waals potentials; checking this explicitly is beyond the scope of this work. If this assertion is correct, then the experimentally determined value of $\bar{a}^{(2)}/r_6$ for Cs cannot be fully explained by the single-channel van der Waals theory. Interestingly, the value for $[\bar{a}^{(1)}/\bar{a}^{(2)}]^{-1}$ reported in Table 2 is in agreement with that obtained for a coupled-channel theory model in the limit of negligible closed-channel contribution [34]. The lithium data are for a three-spin system and the determination of $\bar{a}^{(1)}$ is expected to be—according to the paper [36] that analyzed the experimental data—"compromised" by the fact that the three s-wave scattering lengths are slightly different. Interestingly, though, the value of $\bar{a}^{(2)}/r_6$ agrees with what is reported in Table 2.

We conclude by re-emphazising that the structural properties provide a great deal of insight. If the quantum mechanical probability densities of alkali trimers could be imaged, as those of the helium trimers have been, that would provide tremendous additional insight.

Acknowledgements DB gratefully acknowledges stimulating discussions with R. Dörner, M. Kunitski, and Y. Yan and support through the National Science Foundation through Grant No. PHY-1205443.

References

1. Efimov V (1970) Energy levels arising from resonant two-body forces in a three-body system. Phys. Lett. B 33:563-564
2. Lim T K, Duffy S K, Damer W C (1977) Efimov State in the ^{4}He Trimer. Phys. Rev. Lett. 38:341-343
3. Cornelius T, Glöckle W (1986) Efimov states for three ^{4}He atoms?. J. Chem. Phys. 85:3906-3912
4. Bedaque P F, Hammer H-W, van Kolck U (1999) Renormalization of the Three-Body System with Short-Range Interactions. Phys. Rev. Lett. 82:463-467
5. Nielsen E, Macek J H (1999) Low-Energy Recombination of Identical Bosons by Three-Body Collisions. Phys. Rev. Lett. 83:1566-1569
6. Esry B D, Greene C H, Burke J P (1999) Recombination of Three Atoms in the Ultracold Limit. Phys. Rev. Lett. 83:1751-1754
7. Bedaque P F, Braaten E, Hammer H-W (2000) Three-body Recombination in Bose Gases with Large Scattering Length. Phys. Rev. Lett. 85:908-911

8. Braaten E, Hammer H-W (2006) Universality in few-body systems with large scattering length. Physics Reports 428:259-390
9. Ferlaino F, Grimm R (2010) Trend: Forty years of Efimov physics: How a bizarre prediction turned into a hot topic. Physics 3:9
10. Kraemer T, Mark M, Waldburger P, Danzl J G, Chin C, Engeser B, Lange A D, Pilch K, Jaakkola A, Nägerl H-C, Grimm R (2006) Evidence for Efimov quantum states in an ultracold gas of caesium atoms. Nature 440:315-318
11. Knoop S, Ferlaino F, Mark M, Berninger M, Schöbel H, Nägerl H-C, Grimm R (2009) Observation of an Efimov-like trimer resonance in ultracold atomdimer scattering. Nature Phys. 5:227-230
12. Zaccanti M, Deissler B, D'Errico C, Fattori M, Jona-Lasinio M, Müller S, Roati G, Inguscio M, Modugno G (2009) Observation of an Efimov spectrum in an atomic system. Nature Phys. 5:586-591
13. Gross N, Shotan Z, Kokkelmans S, Khaykovich L (2009) Observation of Universality in Ultracold ^{7}Li Three-Body Recombination. Phys. Rev. Lett. 103:163202
14. Pollack S E, Dries D, Hulet R G (2009) Universality in Three- and Four-Body Bound States of Ultracold Atoms. Science 326:1683-1685
15. Ottenstein T B, Lompe T, Kohnen M, Wenz A N, Jochim S (2008) Collisional Stability of a Three-Component Degenerate Fermi Gas. Phys. Rev. Lett. 101:203202
16. Huckans J H, Williams J R, Hazlett E L, Stites R W, O'Hara K M (2009) Three-Body Recombination in a Three-State Fermi Gas with Widely Tunable Interactions. Phys. Rev. Lett. 102:165302
17. Williams J R, Hazlett E L, Huckans J H, Stites R W, Zhang Y, O'Hara K M (2009) Evidence for an Excited-State Efimov Trimer in a Three-Component Fermi Gas. Phys. Rev. Lett. 103:130404
18. Wenz A N, Lompe T, Ottenstein T B, Serwane F, Zürn G, Jochim S (2009) Universal trimer in a three-component Fermi gas. Phys. Rev. A 80:040702(R)
19. Lompe T, Ottenstein T B, Serwane F, Wenz A N, Zürn G, Jochim S (2010) Radio-Frequency Association of Efimov Trimers. Science 330:940-944
20. Nakajima S, Horikoshi M, Mukaiyama T, Naidon P, Ueda M (2011) Measurement of an Efimov Trimer Binding Energy in a Three-Component Mixture of ^{6}Li. Phys. Rev. Lett. 106:143201
21. Chin C, Grimm R, Julienne P, Tiesinga E (2010) Feshbach resonances in ultracold gases. Rev. Mod. Phys. 82:1225-1286
22. Berninger M, Zenesini A, Huang B, Harm W, Nägerl H-C, Ferlaino F, Grimm R, Julienne P S, Hutson J M (2011) Universality of the Three-Body Parameter for Efimov States in Ultracold Cesium. Phys. Rev. Lett. 107:120401
23. Roy S, Landini M, Trenkwalder A, Semeghini G, Spagnolli G, Simoni A, Fattori M, Inguscio M, Modugno G (2013) Test of the Universality of the Three-Body Efimov Parameter at Narrow Feshbach Resonances. Phys. Rev. Lett. 111:053202
24. Wang J, D'Incao J P, Esry B D, Greene C H (2012) Origin of the Three-Body Parameter Universality in Efimov Physics. Phys. Rev. Lett. 108:263001
25. Naidon P, Endo S, Ueda M (2014) Physical origin of the universal three-body parameter in atomic Efimov physics. Phys. Rev. A 90:022106
26. Naidon P, Endo S, Ueda M (2014) Microscopic Origin and Universality Classes of the Efimov Three-Body Parameter. Phys. Rev. Lett. 112:105301
27. Wang Y, Julienne P S (2014) Universal van der Waals Physics for Three Ultracold Atoms. Nature Phys. 10:768-773
28. Gogolin A O, Mora C, Egger R (2008) Analytical Solution of the Bosonic Three-Body Problem. Phys. Rev. Lett. 100:140404
29. In the literature, the "Efimov ground state" is often labeled by $n = 0$ instead of $n = 1$ as done here.
30. Thøgersen M, Fedorov D V, Jensen A S (2008) N-body Efimov states of trapped bosons. Europhys. Lett. 83:30012
31. Platter L, Ji C, Phillips D R (2009) Range corrections to three-body observables near a Feshbach resonance. Phys. Rev. A 79:022702
32. D'Incao J P, Greene C H, Esry B D (2009) The short-range three-body phase and other issues impacting the observation of Efimov physics in ultracold quantum gases. J. Phys. B 42:044016
33. Naidon P, Ueda M (2011) The Efimov effect in lithium 6. C. R. Phys. 12:13-26
34. Schmidt R, Rath S, Zwerger W (2012) Efimov physics beyond universality. Eur. Phys. J. B 85:386
35. Horinouchi Y, Ueda M (2015) Onset of a Limit Cycle and Universal Three-Body Parameter in Efimov Physics. Phys. Rev. Lett. 114:025301
36. Huang B, O'Hara K M, Grimm R, Hutson J M, Petrov D S (2014) Three-body parameter for Efimov states in ^{6}Li. Phys. Rev. A 90:043636
37. Voigtsberger J, Zeller S, Becht J, Neumann N, Sturm F, Kim H-K, Waitz M, Trinter F, Kunitski M, Kalinin A, Wu J, Schöllkopf W, Bressanini D, Czasch A, Williams J B, Ullmann-Pfleger K, Schmidt L P H, Schöffler M S, Grisenti R E, Jahnke T, Dörner R (2014) Imaging the structure of the trimer systems $^4He_3$ and $^3He^4He_2$. Nature Communications 5:5765
38. Kunitski M, Zeller S, Voigtsberger J, Kalinin A, Schmidt, L P H Schöffler M, Czasch A, W. Schöllkopf W, Grisenti R E, Jahnke T, Blume D, Dörner R (2015) Observation of the Efimov state of the helium trimer. Science 348:551-555
39. Esry B D, Lin C D, Greene C H (1996) Adiabatic hyperspherical study of the helium trimer. Phys. Rev. A 54:394-401

40. Nielsen E, Fedorov D V, Jensen A S (1998) The structure of the atomic helium trimers: halos and Efimov states. J. Phys. B 31:4085-4105
41. Naidon P, Hiyama E, Ueda M (2012) Universality and the three-body parameter of ^{4}He trimers. Phys. Rev. A 86:012502
42. Even though the ground state of the helium trimer is not a true Efimov state, it exhibits universal characteristics that are typical for weakly-bound trimer systems (see, e.g., Refs. [43; 44; 45]).
43. Braaten E, Hammer H-W (2003) Universality in the three-body problem for ^{4}He atoms. Phys. Rev. A 67:042706
44. Delfino A, Frederico A, Tomio L (2000) Low-energy universality in three-body models. Few-Body Systems 28:259-271
45. Yamashita M T, de Carvalho R S M, Tomio L, Frederico T (2003) Scaling predictions for radii of weakly bound triatomic molecules. Phys. Rev. A 68:012506
46. Cencek W, Przybytek M, Komasa J, Mehl J B, Jeziorski B, Szalewicz K (2012) Effects of adiabatic, relativistic, and quantum electrodynamics interactions on the pair potential and thermophysical properties of helium. J. Chem. Phys. 136:224303
47. Przybytek M, Cencek W, Komasa J, Lach G, Jeziorski B, Szalewicz K (2012) Relativistic and Quantum Electrodynamics Effects in the Helium Pair Potential. Phys. Rev. Lett. 104:183003
48. Gonzáles-Lezana T, Rubayo-Soneira J, Miret-Artés S, Gianturco F A, Delgado-Barrio G, Villarreal P (1999) Efimov States for ^{4}He Trimers?. Phys. Rev. Lett. 82:1648
49. Hiyama E, Kamimura M (2014) Universality in Efimov-associated tetramers in ^{4}He. Phys. Rev. A 90:052514
50. Kievsky A, Gattobigio M (2013) Universal nature and finite-range corrections in elastic atom-dimer scattering below the dimer breakup threshold. Phys. Rev. A 87:052719
51. Blume D, Greene C H, Esry B D (2000) Comparative study of He_3, Ne_3, and Ar_3 using hyperspherical coordinates. J. Chem. Phys. 113:2145-2158; see also Blume D, Greene C H, Esry B D (2014) Erratum. J. Chem. Phys. 141:069901
52. Lin C D (1995) Hyperspherical coordinate approach to atomic and other Coulombic three-body systems. Phys. Rep. 257:1-83
53. Fedorov D V, Jensen A S (1993) Efimov effect in coordinate space Faddeev equations. Phys. Rev. Lett. 71:4103-4106.
54. Jonsell S, Heiselberg H, Pethick C J (2002) Universal Behavior of the Energy of Trapped Few-Boson Systems with Large Scattering Length. Phys. Rev. Lett. 89:250401
55. It is imperative, though, to realize that both the $n = 1$ and 2 states are extremely diffuse with a wide range of configurations having non-zero probability.
56. The effective range is about 3 times larger than r_6, implying that $\langle R \rangle \approx 1.5 r_e$.
57. The zero-range theory wave function for finite a can be calculated numerically; this is, however, not pursued in this work. It is reasonable to assume that the finite a cos-distributions obtained from the zero-range theory agree very well with the finite-range $n = 2$ distributions shown in Figs. 4 and 5.
58. Huang B, Sidorenkov L A, Grimm R, Hutson J M (2014) Observation of the Second Triatomic Resonance in Efimov's Scenario. Phys. Rev. Lett. 112:190401